J Mater Sci (2011) 46:4858–4863
DOI 10.1007/s10853-011-5397-8

Effective electron emitters by molybdenum oxide-coated carbon nanotubes core–shell nanostructures

Jun Yu · Daniel H. C. Chua

Received: 24 November 2010 / Accepted: 12 February 2011 / Published online: 24 February 2011

Abstract In this article, we showed that simple metal oxide coatings such as MoO_3 can be an effective enhancer for carbon nanotubes (CNTs) in field emission (FE) performance. For comparison, the FE properties of the pristine vertically aligned multi-walled CNTs with the metal oxide-coated CNTs were investigated. The metal oxide coating of the pristine CNTs was carried out by metal–organic chemical vapor deposition (MOCVD) method at 400 °C using $Mo(CO)_6$ as the precursor. The core–shell structure of the nanocomposite was studied by transmission electron microscopy (TEM). X-ray photoelectron spectroscopy (XPS) results showed that the surface of the coating material was mainly MoO_3. FE test indicated that the MoO_3-coated CNTs film exhibited an enhanced performance than the pristine CNTs with a turn-on field of 1.33 V μm^{-1} and a field enhancement factor β estimated to be $\sim$7000. Ultraviolet photoelectron spectroscopy (UPS) results confirmed a lower electron emission barrier height for MoO_3-coated CNTs than for the pristine CNTs. The mechanism of the enhanced FE performance is discussed based on Schottky barrier effect.

Introduction

Carbon nanotubes (CNTs) have attracted great interest due to their remarkable thermal, mechanical, and electronic properties, such as high thermal conductivity, high stiffness, high Young's modulus, and high current density [1, 2]. These superior properties make them candidates for a wide range of applications, including chemical sensors, field emission (FE) materials, catalyst support, nanoelectronic devices, strength reinforcements in high performance composites, electrode for lithium ion in batteries, and hydrogen storage [3, 4]. The enviable properties, such as nanometer-sized diameter, structural integrity, high electrical and thermal conductivity, and chemical stability, make CNTs excellent electron emitters, which leads to potential applications in flat panel displays [5–7]. In the past couple of years, researchers have tried various methods to improve the FE performance of CNTs for such electron emission applications. The key criterion in this application is to synthesize large arrays of well-aligned CNTs on both glass and silicon substrates [8, 9]. Several methods for improving FE have been explored. One method starts with the fabrication of metal tips on which CNTs were grown directly on the tip to achieve a lower voltage supply for emission and more stable emission characteristics [10, 11]. Another method includes modifying the proximity of neighboring CNTs to find the optimal density coverage for CNTs that could reduce or eliminate field-screening effects [12]. Currently, patterned CNTs produced using lithography technique may produce the best electron emission properties. However, this technique, usually through the use of electron beam lithography, is costly and do faces difficulty in the production of large area displays. As such, this limits its adoption by the industry [13–16].

Recently, some researchers started exploring alternative techniques that modify the CNTs using surface-coating method to achieve better FE performance. Zhang et al. demonstrated that hafnium carbide (HfC) coated on the surface of CNTs led to improved FE current density, emission uniformity, and emission stability. This core–shell

J. Yu · D. H. C. Chua (✉)
Department of Materials Science and Engineering, National University of Singapore, 7 Engineering Drive 1, Singapore 117574, Singapore
e-mail: msechcd@nus.edu.sg

structure was first obtained by coating Hf metal on pristine CNTs and annealing the composite at 1200 °C [17]. Uh et al. [18] coated titanium (Ti) over the surface of CNTs, under different film thickness, and reported that thin Ti-coated CNTs with thickness of 10 nm or less showed enhanced FE properties as compared with pristine CNTs. There are attempt to use CNTs itself as a coating material to enhance the FE performance of the pristine CNTs substrate by a secondary growth approach [19]. Other research groups have reported coating the CNT surface with wide bandgap materials (WBGMs) such as SiO_2, MgO, and BN and observed lower turn-on field and higher field enhancement [20, 21]. The enhanced FE performance is probably due to the negative electron affinity (NEA) of these coating materials, which may help to decrease the effective emission barrier height of the emitters thus allowing electron emission at a lower turn-on electric field. Molybdenum (metal) is a well-known material widely used for electron emission. It has been reported to be a good emitter but can be easily eroded during the emission process. However, molybdenum oxide is a wide bandgap n-type semiconductor (Eg $\sim$ 3.15 eV) and possesses excellent corrosion resistance [22]. Recently, there have been considerable studies reporting on the FE properties of molybdenum oxide, including both MoO_3 and MoO_2 in the form of nanobelts, nanostars, and nanowires [23–26]. In this article, we demonstrate that through the use of suitable materials, such as metal oxide and specifically MoO_3, the turn-on field for the metal oxide-coated CNTs will be significantly reduced. The mechanism behind the enhanced FE performance of the metal oxide-coated CNTs is believed to be attributed to the Schottky barrier effect.

Experimental procedure

Coating of CNTs was carried out using a custom-designed metal–organic chemical vapor deposition (MOCVD) system with a rapid-heating induction generator. High density vertically aligned CNTs were used as the substrates, which were obtained using Fe catalyst and after 20 min growth in a plasma-enhanced chemical vapor deposition (PECVD) chamber, the average length of the CNTs was about 14.4 μm. The growth conditions for the CNTs are 700 °C with 1.2 Torr C_2H_2 as the feed gas. $Mo(CO)_6$ was used as the MOCVD precursor (bought from Sigma-Aldrich Pte Ltd, 99.0%). The whole MOCVD system was vacuumed to $\sim 10^{-6}$ Torr after the substrates were mounted at the center of the quartz tube (42 mm in diameter and 400 mm in length). The solid $Mo(CO)_6$ precursor was vaporized by heating the bubbler to approximately 60 °C and carried to the reaction chamber (quartz tube) by Ar gas at a flow rate of 100 sccm. The deposition was conducted by maintaining the chamber pressure at $\sim 10^{-2}$ Torr while rapidly heating the substrate to 400 °C within 2 min. The temperature was maintained for a further 2 min without changing the conditions. The MOCVD system was cooled down to room temperature in Ar ambient to prevent further oxidation.

Vacuum FE tests of the pristine and coated CNTs samples were carried out using a custom-designed parallel plate geometry FE system at room temperature. For each test, the emitter-to-anode distance was maintained at 100 μm by inserting a polymer film spacer, on which a hole with a fixed area was fashioned to define the total emission area. The spacer was placed on top of the samples to make sure the distance between the emitters and the anode was kept constant. Two clips were used to fix the position of the anode and spacer. The clips were controlled to be just tight enough to prevent sliding of the spacer but not too tight to press or distort the spacer. The chamber was pumped down to a base pressure of 1.0×10^{-6} Torr. The FE current–voltage (I–V) relationship was obtained by applying a dc field between the sample and anode. Emission current was measured using a Keithley 237 source measurement unit.

In order to better understand the FE enhancement mechanism, the samples were studied by scanning electron microscopy (SEM), X-ray photoelectron spectroscopy (XPS), ultraviolet photoelectron spectroscopy (UPS), and transmission electron microscopy (TEM). A Phillips XL30-FEG (Field Emission Gun) SEM equipped with an Ion Getter Pump (IGP), which enables the normal working pressure for the source to achieve about 2×10^{-9} Torr or better was used. Both XPS and UPS analysis were carried out using a Kratos DLD Ultra UHV spectrometer. A monochromatized Al Kα X-ray source (1486.6 eV photons) with a spot size of about 1 mm was used for XPS measurements. Core-level XPS spectra were obtained by photoelectrons at a take-off angle of 90°, measured with respect to the sample surface at a vacuum of 5×10^{-9} Torr. For UPS, photons of the He(I) resonance line (21.2 eV) through a helium cold discharge were used. XPS spectra were collected in a concentric hemispherical analyzer in a constant energy mode, with a pass energy E_p of 20 eV. In the case of UPS, the analyzer energy was set to 120 meV with the acquisition time per spectrum $\sim$150 s. A high-resolution TEM (JEOL-2010F) operating at 200 kV was used to obtain the nanostructure of the samples.

Results and discussion

The turn-on field for FE performance is defined as the field that required to achieve an emission current density of 10 μA cm^{-2} [27–29]. Figure 1 showed the current density–electric field (J–E) curves for both the pristine CNTs and the coated CNTs samples. It can be observed that the

turn-on field for the pristine CNTs was 2.34 V μm^{-1} whereas for the film-coated CNTs was 1.33 V μm^{-1}. The turn-on field value for the coated CNTs is significantly lower, suggesting that compared to the pristine CNTs, the coated CNTs material is able to generate higher FE current at lower voltages. Furthermore, it was observed after the onset of electron emission, the *J–E* curve of the film-coated CNTs rises gradually while the curve of the pristine CNTs at a sharper "kink" climbs at a much steeper gradient. The different shapes around the local extrema in inset of Fig. 1a and b may imply that the emission spot of pristine CNTs may occur at the tip (single-point extrema) while for the film-coated CNTs, both the tip and the side-wall emission probably takes place simultaneously thus the change in the extrema shifts towards a curve-like shape. The position of this extrema is linked to a lower turn-on field in the *I–V* plot.

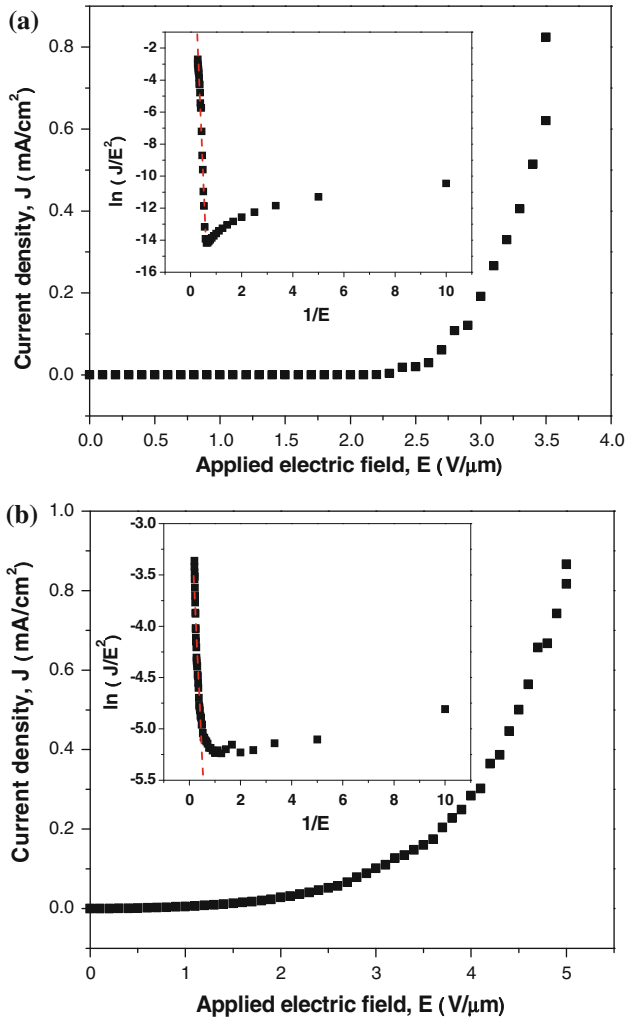

Fig. 1 The field emission *J–E* characteristic of **a** the CNTs film and **b** the MOCVD sample that obtained at 400 °C. Corresponding F–N plots are shown in the inset

The quantitative description of field emitters is usually evaluated using the framework of the Fowler–Nordheim (F–N) theory [30]. According to the F–N theory, the FE current density can be expressed as,

$$J = \frac{\alpha A}{\phi}(\beta E)^2 \exp\left(-\frac{B\phi^{\frac{3}{2}}}{\beta E}\right) \quad (1)$$

where Φ is the barrier height of the emitters (eV), α is the effective emission area, and β is the field enhancement factor. The universal constants $A = 1.54 \times 10^{-6}$ A eV V^{-2} and $B = 6.83 \times 10^3$ $eV^{-3/2}$ V μm^{-1}.

The plots of $\ln(J/E^2)$ versus $1/E$ (so called F–N plot) displayed in the inset of both Fig. 1a and b comprised a linear region, emphasizing the quantum tunneling electron emission mechanism. By transforming Eq. 1, the slope of the linear region of the F–N plot can be expressed as

$$\text{Slope} = -6.83 \times 10^3 \frac{\phi^{\frac{3}{2}}}{\beta} \quad (2)$$

The value of the slope can be obtained by fitting the F–N curve to the experimental results. Hence, the β factor can be calculated through Eq. 2 if only the barrier height value Φ was known.

In order to further study the FE properties of these samples, UPS technique was employed to measure their electron emission barrier height values at room temperature. Figure 2 showed the UPS spectra for both the pristine and the film-coated CNTs samples. The spectra measurement showed that the electron emission barrier height for film-coated CNTs was approximately 3.65 eV and for pristine CNTs was around 4.70 eV. The electron emission barrier height obtained for the pristine CNT was consistent

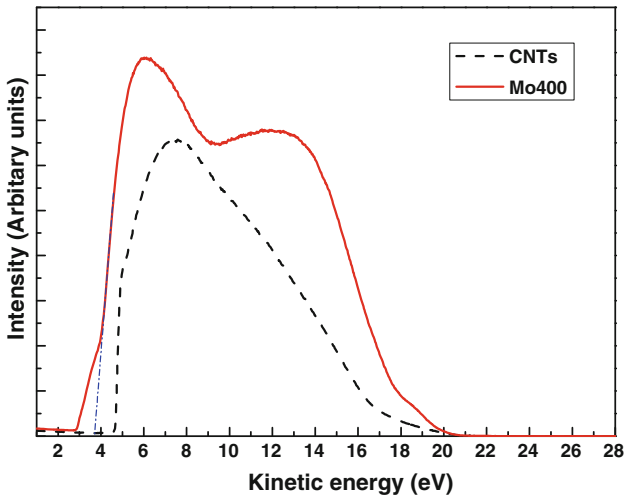

Fig. 2 UPS spectra of pristine CNTs (*dash line*) and MoO_3-coated CNTs (*solid line*). The extrapolation (*dash dot line*) of the coated CNTs curve (Kinetic energy from 3.97 to 4.98 eV) on to *x*-axis gives its electron emission barrier height

with previous reports by other researchers [31–33]. Substituting these two values into Eq. 2 gave the β factors, those were ~7000 for film-coated CNTs whereas ~1800 for the pristine CNTs. The results indicate that the coated CNTs sample possessed enhanced FE characteristics better than the reference pristine CNTs film and improved performance as compared with some recently reported inorganic nanostructure emitters, such as ZnS, WO_3, CdS, SnO_2, GaAs, etc [20, 21, 34].

Figure 3 showed the top view and cross-section view SEM images of the pristine and film-coated CNTs samples. It can be observed in Fig. 3c and d that a layer of whiskers were formed at the upper to topmost tip of CNTs and these whiskers seemed to extend from the tip of CNTs. Some of the whiskers were extraordinary straight and protruding out, together with other curly ones. As these different protrusions may induce a larger local field at the tips [35], it is highly likely that side-walled emissions may occur simultaneously with the tip emissions and thus leading to a different *J–E* curve observed from pristine CNTs. In order to ensure a uniform electron emission across the entire specimen surface, a phosphorus-coated screen was used in the experiment as an anode. We observed uniform emission throughout the phosphors screen during the FE test and not a few emission dots.

To verify our theory, XPS technique was used to investigate the bonding state of the coated material. Figure 4 showed the high-resolution XPS spectrum of Mo 3d peaks from the coated CNT sample. The spectrum showed a peak located at binding energy of 229.4 eV which was due to Mo^{4+} oxide species, while that at 232.6 eV was due to a Mo^{6+} oxide species, indicating that the film surface was composed of a large quantity of MoO_3 and also some MoO_2. At a lower binding energy of 230.5 eV was assigned to the Mo_2C peak, suggesting that the critical Mo-C type of bond is possibly formed and/or is present at the interface between the CNTs and MoO_3, which implies the formation of Schottky contact for electron diffusion. The intensity of the Mo_2C peak is very much lower than the oxide peaks thus hinting that only bond formation is present and not a Mo_2C thin layer.

MoO_2 and Mo_2C were believed to be obtained during the deposition process. As reported by Chen et al. [36], $Mo(CO)_6$ has been widely used in the growth of Molybdenum films at temperature of ~300 °C with the reaction shown as below:

$$Mo(CO)_6 \rightarrow Mo + 6CO$$

However, at higher temperatures, such as 400 °C, and at the present of CNTs, the reaction scheme can be postulated as follows:

$$2CO \rightarrow C + CO_2$$

$$2Mo + C \rightarrow Mo_2C$$

$$5Mo + 2CO \rightarrow 2Mo_2C + MoO_2$$

After the reactions above, the surface of the film was believed to be oxidized such that MoO_3 was formed. The carbon linked to the formation of Mo_2C can be attributed to the surface of the CNTs, which are tubes of graphitic carbon.

High-resolution TEM was used to examine the microstructure of the MoO_3-coated CNTs specimen. Figure 5a

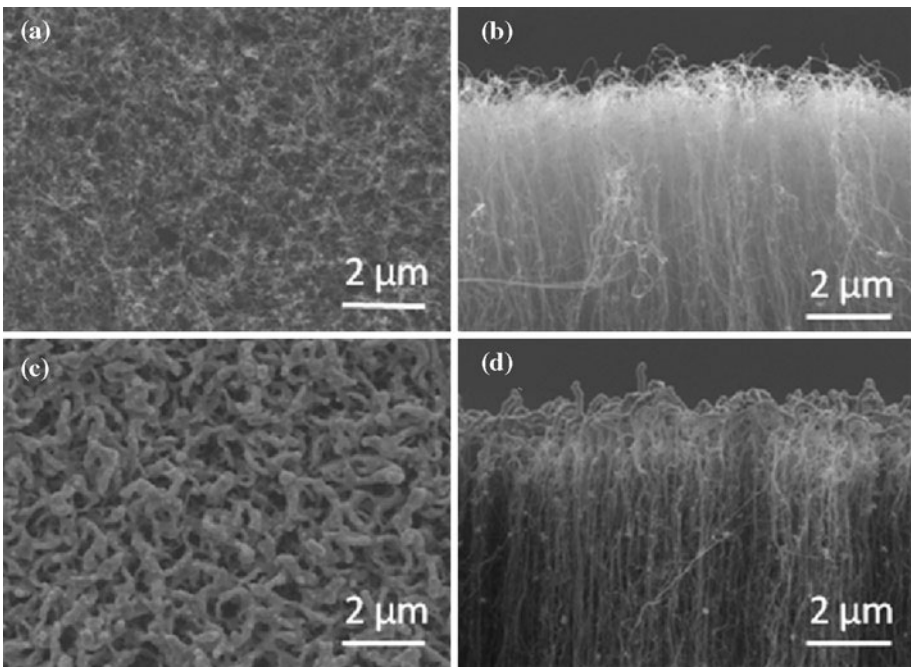

Fig. 3 SEM images of pristine and coated CNTs samples. **a** top view and **b** cross-section view of original CNTs film; **c** top view and **d** cross-section view of coated CNTs film

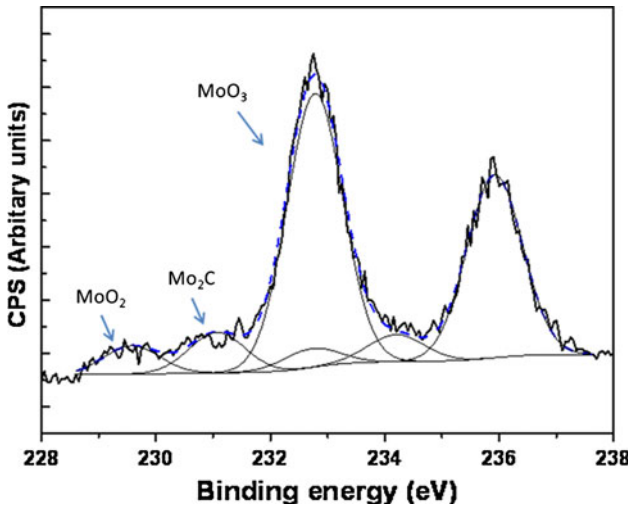

Fig. 4 Mo 3d XPS core-level spectra of the coated CNTs sample that obtained at 400 °C by MOCVD

showed the core–shell structure of the MoO_3-coated CNTs. It can be clearly observed from the TEM image that CNT areas exposed to the CVD process were uniformly wrapped by a layer of nano-particles, which has been confirmed to be MoO_3 particles by XPS. This further confirms that the Mo_2C peak obtained in the XPS peak analysis is due to the interface bonding and not Van de Waals attraction as no separate layers were observed. A schematic band diagram of the composite core–shell material was sketched in Fig. 5b. As shown, it is believed that a Schottky barrier effect was present and electron emission barrier height of coated CNTs was lower than that of the pristine CNTs from our experimental results.

Schottky effect refers to the phenomenon that when a positive voltage is applied to the anode with respect to the cathode, the electric field at the cathode helps the emission process by lowering the potential energy barrier [37]. If the CNTs has certain metal or semiconductor materials directly coated on the surface forming bonds, Schottky-type contacts would be formed, i.e., Schottky barriers would be obtained at the interfaces [38]. Since MoO_3 is a wide bandgap n-type semiconductor ($E_g \sim 3.15$ eV) [22], a Schottky barrier was predicted to be obtained between MoO_3 and CNTs. The presence of the Mo-C type of bonds by XPS confirms the formation of the Schottky contact. As shown in Fig. 5b, due to the applied electric field, electrons and holes would separate, inducing the band bending and hence resulting in a potential drop ΔV across the coating material, which implied that the FE originated from the conduction band of the coating material as well. Electrons would tunnel from near the Fermi energy level of the back contact, i.e., CNT, into the conduction band of the coating material, i.e., MoO_3 thin film. While traversing the MoO_3 thin film as hot electrons, the electrons can tunnel out to the

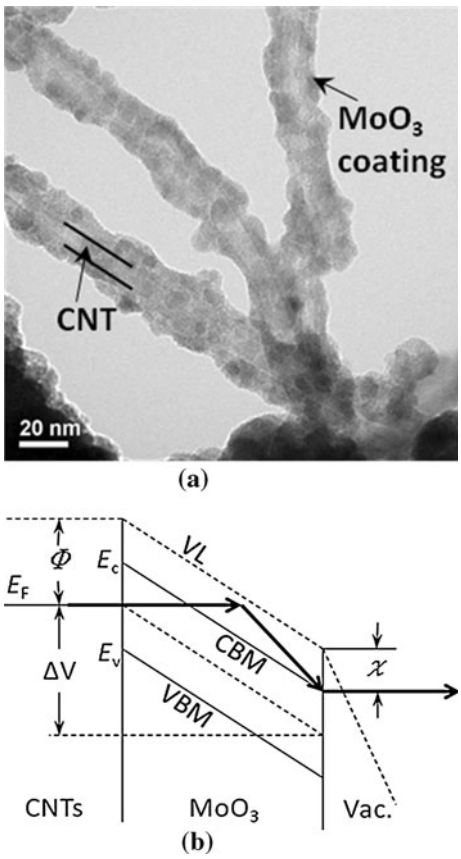

Fig. 5 **a** HR-TEM image of the core–shell nanostructure of the MoO_3-coated CNTs. **b** A schematic band diagram of field emission from coated CNTs thin film to vacuum. Φ represents the electron emission barrier height of CNTs, and χ is the electron affinity of MoO_3. Electrons are injected from the Fermi energy E_F of CNTs to the conduction band of MoO_3. After thermalization to the conduction band minimum (CBM), electrons are emitted at MoO_3/vacuum interface. The potential drop ΔV was induced due to the applied electric field. VL refers to vacuum level and VBM denotes valence band minimum

vacuum at the front surface with an overall lowered emission barrier height than the original height of the pristine CNT [22, 39, 40]. This tunneling process is illustrated by the solid arrow in Fig. 5b, and this is the underlying principle for the FE enhancement of the MoO_3-coated CNTs.

Conclusions

We have investigated the FE characteristics of the pristine and the metal oxide MoO_3-coated CNTs. After coating the CNTs with MoO_3 at 400 °C by MOCVD, the emitters revealed significantly enhanced FE properties than the pristine CNTs with a turn-on field of 1.33 V μm^{-1} and a field enhancement factor β estimated to be $\sim$7000. A possible explanation for the FE enhancement mechanism

is that a Schottky barrier formed at the CNTs/MoO_3 interface, which induced electron injection from the Fermi level of CNTs to the conduction band of MoO_3 followed with FE from the conduction band minimum of MoO_3 to the vacuum. The considerably lowered overall electron emission barrier height increased the electron injection probability and therefore enhanced the FE performance of such composite emitters.

Acknowledgements The authors would like to acknowledge the support from R284000087112 for the research work. Field emission work was performed at NUS Nanoscience & Nanotechnology Initiative (NUSNNI) facilities.

References

1. Popov VN (2004) Mater Sci Eng R Rep 43:61
2. Dragoman M, Dragoman D (2006) Nanoelectronics: principles and devices. Artech house, Inc, Boston
3. Paradise M, Goswami T (2007) Mater Des 28:1477
4. Zhang F, Shen J, Sun J, Zhu YQ, Wang G, McCartney G (2005) Carbon 43:1254
5. Dresselhaus MS, Dresselhaus G, Avouris P (2001) Carbon nanotubes: synthesis, structure, properties, and applications. Springer, Berlin
6. Wang QH, Setlur AA, Lauerhaas JM, Dai JY, Seeling EW, Chang RPH (1998) Appl Phys Lett 72:2912
7. Zhu H, Wei B (2008) J Mater Sci Technol 24:447
8. Ren ZF, Huang ZP, Xu JW, Wang JH, Bush P, Siegal MP, Provencio PN (1998) Science 282:1105
9. Fan S, Chapline MG, Franklin NR, Tombler TW, Cassell AM, Dai H (1999) Science 283:512
10. Zhu J, Mao DJ, Cao AY, Liang J, Wei BQ, Xu CL, Wu DH, Peng ZA, Zhu BH, Chen QL (1998) Mater Lett 37:116
11. Sharma RB, Tondare VN, Joag DS, Govindaraj A, Rao CNR (2001) Chem Phys Lett 344:283
12. Suh JS, Jeong KS, Lee JS, Han I (2002) Appl Phys Lett 80:2392
13. Wong YM, Kang WP, Davidson JL, Choi BK, Hofmeister W, Huang JH (2005) Diam Relat Mater 14:2078
14. Huh Y, Lee JY, Lee CJ (2005) Thin Solid Films 475:267
15. Xua NS, Huq SE (2005) Mater Sci Eng R 48:47
16. Choi GS, Son KH, Kim DJ (2003) Microelectron Eng 66:206
17. Zhang J, Yang C, Wang Y, Feng T, Yu W, Jiang J, Wang X, Liu X (2006) Nanotechnology 17:257
18. Uh HS, Park S, Kim B (2010) Diam Relat Mater 19:586
19. Klinke C, Delvigne E, Barth JV, Kern K (2005) J Phys Chem B 109:21677
20. Yi W, Jeong T, Yu SG, Heo J, Lee C, Lee J, Kim W, Yoo JB, Kim J (2002) Adv Mater 14:1464
21. Su CY, Juang ZY, Chen YL, Leou KC, Tsai CH (2007) Diam Relat Mater 16:1393
22. He T, Ma Y, Cao Y, Yin Y, Yang W, Yao J (2001) Appl Surf Sci 180:336
23. Zhou J, Deng SZ, Xu NS, Chen J, She JC (2003) Appl Phys Lett 83:2653
24. Li YB, Bando Y, Golberg D, Kurashima K (2002) Appl Phys Lett 81:5048
25. Khademi A, Azimirad R, Zavarian AA, Moshfegh AZ (2009) J Phys Chem C 113:19298
26. Zhou J, Xu NS, Deng SZ, Chen J, She JC, Wang ZL (2003) Adv Mater 15:1835
27. Chen YS, Huang JH, Hu JL, Yang CC, Kang WP (2007) Carbon 45:3007
28. Zhao B, Yadian B, Chen D, Xu D, Zhang Y (2008) Appl Surf Sci 255:2087
29. Singh BK, Cho SW, Bartwal KS, Hoa ND, Ryu H (2007) Solid State Commun 144:498
30. Cheng Y, Zhou O (2003) Comptes Rendus Math 4:1021
31. Shiraishi M, Ata M (2001) Carbon 39:1913
32. Gao R, Pan Z, Wang ZL (2001) Appl Phys Lett 78:1757
33. Liu P, Sun Q, Zhu F, Liu K, Jiang K, Liu L, Li Q, Fan S (2008) Nano Lett 8:647
34. Fang X, Bando Y, Gautam UK, Ye C, Golberg D (2008) J Mater Chem 18:509
35. Nilsson L, Groening O, Emmenegger C, Kuettel O, Schaller E, Schlapbach L, Kind H, Bonard JM, Kern K (2000) Appl Phys Lett 76:2071
36. Chen HY, Chen L, Lu Y, Hong Q, Chua HC, Tang SB, Lin J (2004) Catal Today 96:161
37. Kasap SO (2006) Principles of electronic materials and devices, 3rd edn. McGraw-hill companies, Boston
38. Appenzeller J, Knoch J, Martel R, Derycke V, Wind S, Avouris P (2002) Electron Devices Meeting, 2002. IEDM '02. Digest. International 8–11:285
39. Schlesser R, McCarson BL, McClure MT, Sitar Z (1997) Vacuum Microelectronics Conference, 1997. Technical Digest., 1997 10th International. 17–21:141
40. Silva SRP, Carey JD, Guo X, Tsang WM, Poa CHP (2005) Thin Solid Films 482:79